INTERFACE

rsif.royalsocietypublishing.org

Review

Cite this article: Milton RD, Minteer SD. 2017 Direct enzymatic bioelectrocatalysis: differentiating between myth and reality. *J. R. Soc. Interface* **14**: 20170253. http://dx.doi.org/10.1098/rsif.2017.0253

Received: 4 April 2017
Accepted: 30 May 2017

Subject Category:
Reviews

Subject Areas:
bioenergetics, biochemistry, biomimetics

Keywords:
direct electron transfer, biofuel cell, biosensor, bioelectrochemistry

Author for correspondence:
Shelley D. Minteer
e-mail: minteer@chem.utah.edu

THE ROYAL SOCIETY PUBLISHING

Direct enzymatic bioelectrocatalysis: differentiating between myth and reality

Ross D. Milton and Shelley D. Minteer

Department of Chemistry, University of Utah, 315 S 1400 E, Room 2020, Salt Lake City, UT 84112, USA

RDM, 0000-0002-2229-0243; SDM, 0000-0002-5788-2249

Enzymatic bioelectrocatalysis is being increasingly exploited to better understand oxidoreductase enzymes, to develop minimalistic yet specific biosensor platforms, and to develop alternative energy conversion devices and bioelectrosynthetic devices for the production of energy and/or important chemical commodities. In some cases, these enzymes are able to electronically communicate with an appropriately designed electrode surface without the requirement of an electron mediator to shuttle electrons between the enzyme and electrode. This phenomenon has been termed direct electron transfer or direct bioelectrocatalysis. While many thorough studies have extensively investigated this fascinating feat, it is sometimes difficult to differentiate desirable enzymatic bioelectrocatalysis from electrocatalysis deriving from inactivated enzyme that may have also released its catalytic cofactor. This article will review direct bioelectrocatalysis of several oxidoreductases, with an emphasis on experiments that provide support for direct bioelectrocatalysis versus denatured enzyme or dissociated cofactor. Finally, this review will conclude with a series of proposed control experiments that could be adopted to discern successful direct electronic communication of an enzyme from its denatured counterpart.

1. Introduction

Oxidoreductase enzymes are biocatalytic proteins that catalyse the coupled oxidation and reduction in two substrates; thus, transferring an electron(s) between the two substrates with the involvement of the cofactor of the enzyme. While multiple mechanisms of biocatalysis and the transfer of electrons exist, figure 1*a* illustrates a commonly adopted mechanism by which both enzymatic substrates bind to the protein. In the case of enzymatic bioelectrocatalysis, the second substrate of the enzyme is replaced with an electrode, so that the catalytic oxidation of the first substrate of the enzyme can supply electrons to the electrode (bioelectrocatalytic oxidation). Conversely, the electrode can be used to reduce an enzyme and ultimately facilitate enzymatic reduction in the second substrate (bioelectrocatalytic reduction). Electron transfer (ET) to an enzyme, however, is most commonly not trivial (especially when the redox cofactor is deeply buried within the protein) and a small electron mediator is employed to facilitate ET (figure 1*b*). In some cases, enzymes are able to undergo ET directly with an electrode surface (figure 1*c*) [1].

The ability to electronically contact an oxidoreductase enzyme has resulted in a wealth of research pertaining to enzymatic fuel cells (EFCs), amperometric biosensors and bioelectrosynthetic devices as well as mechanistic studies of oxidoreductase activity such as inhibition [2–7]. EFCs are devices that use the bioelectrocatalytic capabilities of enzymes to oxidize and reduce substrates in the production of electrical energy [2]. The most common EFCs use O_2-reducing enzymes for the cathodic reaction (producing H_2O by a $4e^-$ reduction), whereas saccharide-, molecular hydrogen (H_2)- or alcohol-oxidizing enzymes are frequently used for the anodic reaction [8–13]. Saccharide/O_2 EFCs have the added benefit of their potential implantation into living hosts that circulate saccharides (such as glucose) or produce lactate or glucose externally, including mammals and insects [14–19].

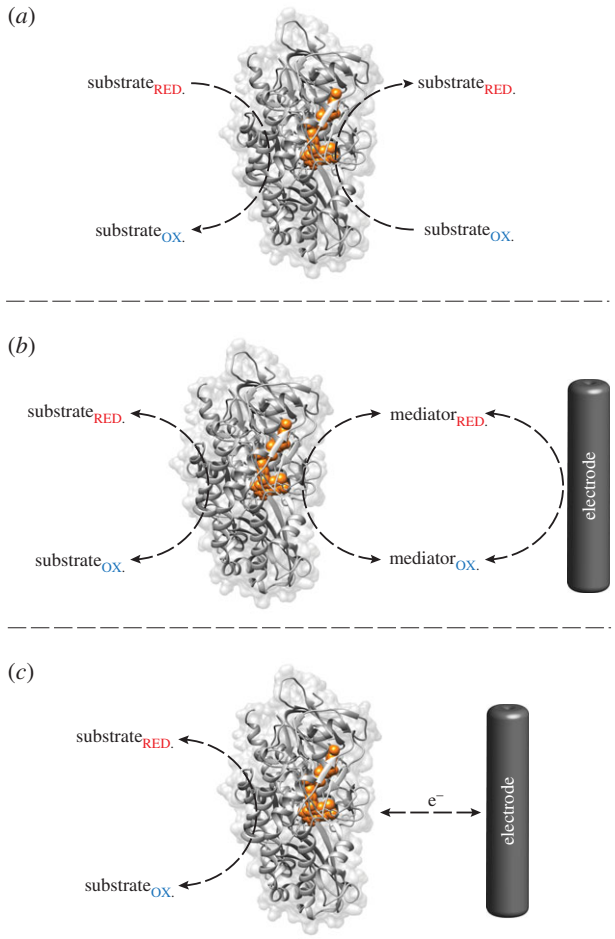

Figure 1. (*a*) Simplified mechanism for the oxidation and reduction of two substrates by an oxidoreductase (grey) with its redox cofactor highlighted in orange. (*b*) MET of bioelectrochemical oxidation or reduction of a substrate by an oxidoreductase. (*c*) DET of bioelectrochemical oxidation or reduction in a substrate by an oxidoreductase. (Online version in colour.)

The inherent substrate specificity of enzymes coupled with their ability to undergo heterogeneous electronic communication with electrodes has also spurred significant research towards creating biosensors for the detection of physiological glucose [20]. Progressing through several developments of electronic communication strategies with oxidoreductases, glucose is now most commonly sensed by the use of an electron mediator that is covalently grafted onto a polymer support, which is also conveniently used to immobilize the enzyme at the electrode surface [21]. The combination of low potential redox mediators and high-specificity enzymes permits the detection of glucose at potentials where other physiological components are seldom interferents (such as ascorbic acid and acetaminophen/paracetamol).

In contrast with EFCs and biosensors that typically produce electrical energy in the presence of substrate/analyte, bioelectrosynthetic systems have been explored, whereby oxidoreductase enzymes are used to convert common substrates into more valuable chemical commodities by the consumption of electrical energy. Most commonly, CO_2 reduction has been explored with the aim of producing formate or alkanes/alcohols, although NAD^+ reduction to NADH is frequently attempted where NAD-dependent enzymes can support reductive reactions [22–24]; Vincent and co-workers [25] have also demonstrated that the coimmobilization of hydrogenase and NAD^+-reducing proteins onto conductive particles can facilitate H_2-driven NADH production. Recent research has also explored the possibility of reducing dinitrogen (N_2) to an important chemical commodity, ammonia (NH_3), while simultaneously producing electrical energy [26].

2. Electron transfer mechanisms

2.1. Mediated electron transfer

As illustrated in figure 1*b*, enzymes are able to use small electroactive molecules to undergo mediated ET (MET) with an electrode, although some prerequisites are necessary to establish electronic communication. First, the electronic properties of the electron mediator must align with the desired bioelectrocatalytic reaction. In the case of oxidative MET, the reduction potential of the mediator should be more positive than the reduction potential of the redox cofactor of the enzyme to enable spontaneous MET (equation (2.1)). The opposite is true of reductive MET, where the reduction potential of the mediator should be more negative than that of the redox cofactor to enable its reduction and subsequent reduction in the substrate. While the optimal magnitude of potential difference between the mediator and redox cofactor has been reviewed to be somewhere between 50 and 170 mV, the reaction quotient defines the cell potential (as per the Nernst equation, equation (2.2)) and must also be considered [2]. The reaction quotient becomes more important when MET can support pseudo-reversible enzymatic MET, as in the case of some hydrogenases where reductive and oxidative catalytic responses can be observed in the same experiment using the same mediator.

$$\Delta G = -nFE_{\text{emf}} \tag{2.1}$$

and

$$E = E^{0'} + \frac{RT}{nF}\ln\frac{[O]}{[R]}, \tag{2.2}$$

where G is the Gibbs free energy, n the number of electrons, F the Faraday constant, E_{emf} the potential in terms of electromotive force (between the enzyme's cofactor and electron donor/acceptor), E the potential of the cell, $E^{0'}$ the formal potential of the species, R the gas constant, T the absolute temperature, O the oxidized species and R the reduced species.

Once a series of electron mediators with suitable electronic properties has been selected, they must next be screened for their ability to interact with the enzyme in a similar fashion to a substrate; this has greater importance in cases where the redox cofactor is deeply buried within the protein structure. We recently demonstrated that naphthoquinone derivatives were able to undergo efficient MET with one type of glucose oxidizing enzyme, while another species did not exhibit any activity even though the enzymes possess the same redox cofactor where their potentials are expected to have negligible effect on the required overpotential of MET, reemphasizing the importance of cofactor accessibility by the electron mediator [27].

2.2. Direct electron transfer

In contrast with MET, some oxidoreductases are able to undergo ET with an electrode surface without the need of an exogenous electron shuttle, where the process is termed

direct ET (DET, as illustrated in figure 1*c*) [1,28]. Typically, a/the redox cofactor of the enzyme is proximal to the electrode, so that efficient heterogeneous ET can take place, where the distance of the redox cofactor from the electrode surface should not exceed 20 Å (2 nm) [2,29].

For the purpose of this review and as most commonly found in the relevant literature, ET is considered to be DET in the sense of direct bioelectrocatalysis if the process meets the following criteria: (i) the redox cofactor(s) of the enzyme remain bound or associated with the enzyme during ET, (ii) ET is not mediated (in the electrochemical sense of the word) by a non-diffusive and/or synthetic electroactive species on the enzyme or electrode surface, and (iii) substrate oxidation/reduction can be observed upon its addition to the system. By applying these criterions, nicotinamide adenine dinucleotide-(NAD) dependent enzymes are not considered to undergo DET, as the NAD cofactor is freely diffusing and not bound to the enzyme. Although we will not consider NAD-dependent enzymes within this review (containing only NAD as the cofactor), it is important to note that researchers have immobilized the NAD cofactor on electrode surfaces, thereby installing a pseudo-DET architecture [30]. There are also naturally occurring enzymes and engineered enzymes that employ an electroactive, non-catalytic subdomain within their protein structure to facilitate DET; this inter-domain ET (IET) pathway will be discussed in the following text.

Since its conception in 1978 where DET between a multicopper oxidase (MCO) (laccase) and a carbon electrode afforded enzymatic O_2 reduction, DET has evolved into an established ET pathway for many oxidoreductases, most commonly (but not limited to) laccase, bilirubin oxidase (BOx), nitrate reductase, hydrogenase and fructose dehydrogenase [31–34].

3. Direct bioelectrocatalysis of metalloenzymes

Many metalloenzymes have been studied by DET and direct bioelectrocatalysis at electrode surfaces. Commonly occurring metallocofactor motifs of such metalloenzymes are: haem centres, iron–sulfur clusters ([Fe–S]), iron (Fe) centres, copper (Cu) centres, molybdenum centres (commonly called Mo-cofactors, Moco) and tungsten, including various iterations and combinations thereof. In many cases, only a single catalytic redox cofactor is found, although others can be found to be involved in internal ET (commonly the case of [4Fe–4S] containing proteins). Frequently, oxidoreductases that contain non-metallocofactors (such as flavin adenine dinucleotide (FAD) and pyrroloquinoline quinone (PQQ)-dependent enzymes) also use metallocofactors to transfer electrons to or from their redox partners, or in our case, electrode surfaces.

MCOs are perhaps the most commonly studied enzymes for direct bioelectrocatalysis, namely laccase and BOx, due to interest in employing them in O_2-reducing EFCs. Typically, MCO enzymes harbour multiple 'types' of Cu centres, termed T1, T2 and T3 (binuclear), where their differences in terminology arise from their coordination numbers, the amino acids to which they are coordinated within enzymes, electron paramagnetic resonance spectroscopic properties and light absorption properties [35–39]. In these MCOs, a T1 site is proximally located and is responsible for single e^- oxidations of their respective substrates (phenolic substrates, bilirubin and ascorbate) and the T2 Cu is combined with the binuclear T3 Cu in a trinuclear cluster (TNC) where O_2 undergoes a $4e^-$ reduction to H_2O once the TNC has been suitably reduced. Figure 2*a* presents a crystal structure of two typical MCOs: laccase (from *Trametes versicolor*) and BOx (from *Myrothecium verrucaria*), where the proximity of the T1 Cu centres to a hypothetical electrode surface can be easily envisaged.

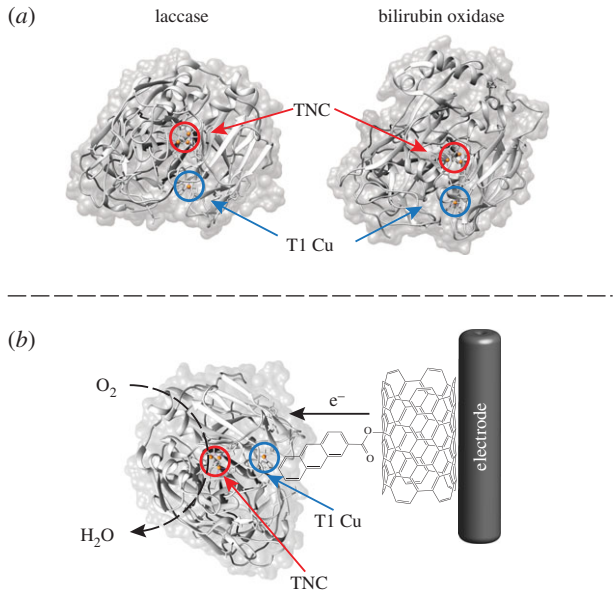

Figure 2. (*a*) Crystal structure of laccase from *T. versicolor* (PDB accession code: 1KYA) and BOx from *M. verrucaria* (PDB accession code: 2XLL). (*b*) Favourable orientation of laccase towards a modified electrode surface for improved direct bioelectrocatalysis. (Online version in colour.)

These MCOs, specifically laccase and BOx, are renowned for their largely orientationally regulated ability to reduce O_2 to H_2O by direct bioelectrocatalysis at electrode surfaces. In the case of laccase, substrate mimics have been shown to greatly improve the catalytic currents that can be observed whereby these mimics promote the orientation of the T1 Cu centre (the electron acceptor of laccase) towards the surface of the electrode, thereby minimizing the distance of electron tunnelling to the T1 centre and improving direct bioelectrocatalysis (figure 2*b*). Typically, polyaromatic hydrocarbons (anthracene, naphthalene and derivatives thereof) are the most commonly employed orientational agents [40–44]. In the case of BOx, efficient DET can be afforded by immobilization onto multi-walled carbon nanotubes, using charged multi-walled carbon nanotubes, immobilized polyaromatic hydrocarbons and even natural substrates (bilirubin and its metabolites) [33,45–49].

Multiple experimental approaches have been adopted to demonstrate that direct bioelectrocatalysis does in fact arise from electronic communication with intact enzymes and not products of their degradation, such as unfolding and/or dissociation of their redox cofactors. Initial experiments usually seek to vary the dissolved O_2 concentration for cyclic voltammetry or steady-state amperometric *i*–*t* analysis, where a direct bioelectrocatalytic current is only observed in the presence of dissolved O_2. The specific orientation and association of laccase and BOx to their substrates or substrate mimics provides strong evidence that the enzyme must remain partially correctly folded (as a minimum). Knowledge surrounding the inhibition of these enzymes by small halide anions has resulted in studies that provide additional experimental evidence to support the argument that O_2 reduction is facilitated by oriented intact enzyme versus dissociated

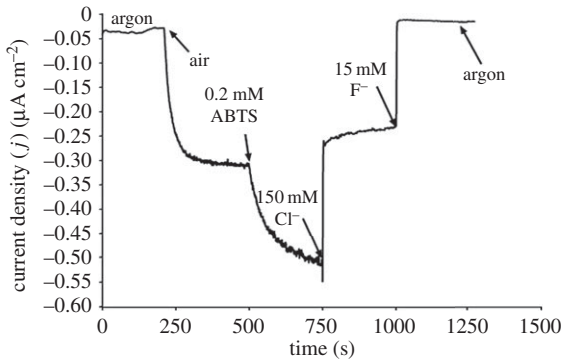

Figure 3. Inhibition of laccase by Cl^- and F^-. Initially, a reductive current is observed for O_2 reduction by laccase undergoing direct bioelectrocatalysis upon the introduction of air. The addition of ABTS (0.2 mM) as an electron mediator results in an increase in the reductive current, due to the establishment of MET with laccase that was not already undergoing DET. The addition of Cl^- (150 mM) results in the loss of MET only, where F^- (15 mM) results in a complete loss of MET and DET. $E_{appl.} = +0.2$ V versus Ag/AgCl (3 M), pH 4.5 citrate/phosphate buffer. Reproduced from [43] with permission from the Royal Society of Chemistry.

cofactor [40,48,50]. Cl^- has been shown to act as a competitive inhibitor to some laccases, competing with substrate inhibition at the T1 Cu centre; thus, electrode architectures designed to possess substrate mimics of laccase are able to out-compete Cl^- inhibition up to 150 mM Cl^-. The addition of F^- as an inhibitor results in the complete loss of direct bioelectrocatalysis (figure 3) [40,48]. Additionally, loadings of laccase onto electrodes at quantities greater than an expected monolayer result in some enzyme that is not orientated, and thus does not undergo direct bioelectrocatalysis. The addition of an additional T1 Cu centre electron mediator (such as ABTS) increases the catalytic current observed on the electrode, due to a mixture of MET and DET pathways. The addition of 150 mM Cl^- typically quenches this additional MET pathway (due to Cl^- competitive inhibition at the T1 Cu centre), providing further evidence for enzymatic orientation [40,48].

Very recently, Dagys *et al.* [51] reported on an efficient laccase bioelectrode whereby ET via the T1 Cu centre was negated altogether and DET was established between an Au electrode and the TNC of the enzyme, achieving high catalytic current densities of nearly 1 mA cm^{-2} (at pH 4). In addition to showing that F^- had a markedly less inhibitory effect on their electrode, where F^- is largely considered to affect ET between the T1 and TNC Cu centres of MCOs, the authors also turned to the use of surface-enhanced Raman spectroscopy and differential spectroelectrochemistry of the T1 and TNC Cu centres to prove that the enzyme was indeed oriented about its TNC.

For many of the scientific reports detailing direct bioelectrocatalysis of MCOs for O_2 reduction at electrode surfaces, enzyme orientation and thus the heterogeneous interfacial ET rate (k_0) is typically considered to be homogeneous and the catalytic reductive current often appears to reach a plateau; however, this is not always the case. Léger *et al.* [52] explored the case where a dispersion of enzyme orientations (a dispersion of k_0 values) results in a catalytic response that does not always reach a plateau within a reasonable potential window. It is important to consider and account for a range of enzyme orientation may be present on an electrode surface when attempting to extrapolate mechanistic and kinetic details.

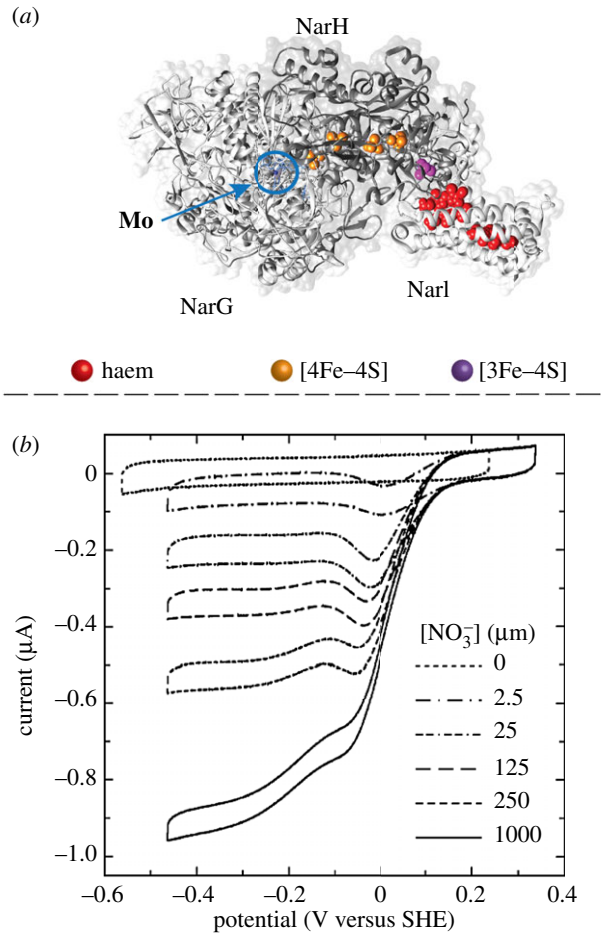

Figure 4. (*a*) Crystal structure of NarGHI NR from *E. coli* (PDB accession code: 1Q16). The haem cofactors are shown in red, the [4Fe–4S] clusters are shown in orange, the [3Fe–4S] cluster is shown in magenta and the Moco is shown in blue. (*b*) Catalytic cyclic voltammogram of NarGHI NR from *E. coli* at a PGE electrode, in the absence or presence of nitrate, where the reductive catalytic current magnitude increases under higher concentrations of nitrate. Experiments were performed at 30°C pH 7.0 on a rotating electrode. Potentials were recorded versus a saturated calomel electrode (SCE) and are reported versus the standard hydrogen electrode (SHE, $E_{SHE} = E_{SCE} + 241$ mV (at 25°C)). The IUPAC convention was used to plot current versus potential, where positive potentials and currents are oxidative [48]. Reprinted (adapted) with permission from [53] (copyright © 2004 American Chemical Society). (Online version in colour.)

Other metalloenzymes are known that possess intricate internal ET pathways, where such an enzyme could function as a transmembrane enzyme (where the enzyme must stretch across and function on either side of a membrane) or the enzyme contains a deeply buried catalytic redox cofactor. One of the most fascinating examples of such an internal ET pathway can be found in prokaryotic nitrate reductase (Nar NR), such as that in *Escherichia coli* (NarGHI NR). Evaluation of this NarGHI NR reveals the protein to be organized as a dimer of heterotrimers (figure 4*a*), harbouring an Mo-dependent cofactor (Moco) in the NarG subunit. Amazingly, this enzyme is able to transfer electrons from its outer haem cofactor (located in the NarI subunit) over a distance of approximately 75 Å (spanning the NarH subunit:, by the way of six internal cofactors that facilitate ET: 1× haem, 4× [4Fe–4S] clusters and 1× [3Fe–4S] cluster [54]. Interest in ET of the different variations of this enzyme (both prokaryotic and eukaryotic) has led to multiple studies of its direct

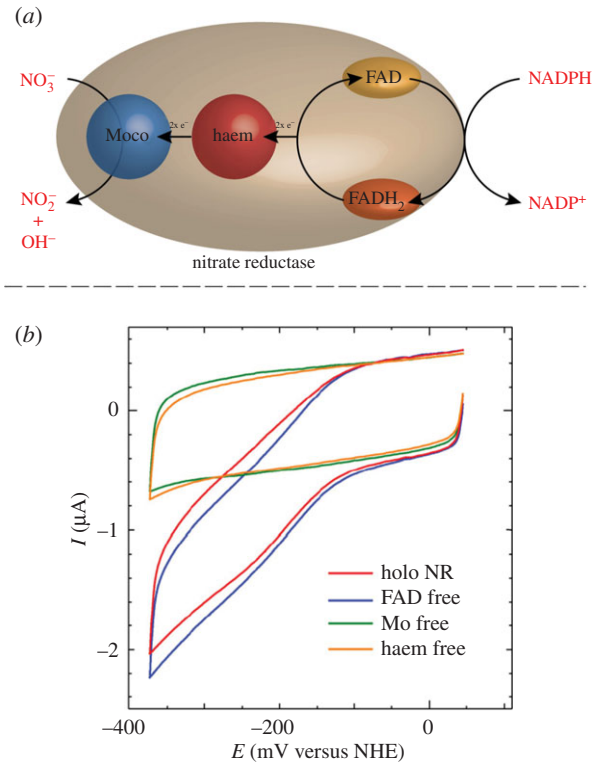

Figure 5. (*a*) Electron flow and catalysis within holo NR from *N. crassa*, as described in [51]. (*b*) Direct bioelectrocatalytic nitrate reduction by holo NR and mutants lacking the Moco, haem or FAD cofactor. Potentials were recorded versus an Ag/AgCl reference electrode and are reported versus the normal hydrogen electrode (NHE, $E_{NHE} = E_{Ag/AgCl} + 196$ mV (at 25°C)). The IUPAC convention was used to plot current versus potential, where positive potentials and currents are oxidative. Reprinted from [51] with permission from Elsevier. (Online version in colour.)

bioelectrocatalysis at electrode surfaces [53,55–58]. Figure 4*b* presents a catalytic cyclic voltammogram for a pyrolytic graphite edge (PGE) electrode modified with NarGHI NR, in the absence and presence of nitrate. In this particular study, the PGE electrode was modified by immersing the electrode into a 10 μM solution of NarGHI NR containing 200 μg ml^{-1} polymyxin, before being rinsed prior to electrochemical testing [53].

A recent study of eukaryotic NR from *Neurospora crassa* from the Bernhardt group investigated the necessity of the different cofactors of this NR for direct bioelectrocatalysis [58]. This NR contains a Moco active site, along with a haem cofactor and an FAD cofactor; NAD(P)H serves as the physiological electron donor of this NR via the FAD cofactor (figure 5*a*). Initially, the authors demonstrated that this NR could directly reduce nitrate (NO_3^-) when immobilized at an electrode surface, although they note that DET was not always obtained and various promoters of DET were used (polymyxin and poly(ethylenimine)) to maintain electrical contact. As the orientation of the enzyme at the electrode surface affects its direct bioelectrocatalysis, this is the first piece of evidence to suggest that direct bioelectrocatalysis is in fact due to immobilized holo-enzyme and not from denatured cofactor. The authors also demonstrated that direct bioelectrocatalysis is only observed when mutants containing the Moco are evaluated, and further, that the haem group is necessary for direct bioelectrocatalysis, whereas the FAD cofactor is not (figure 5*b*). Interestingly, the authors also note that the observed redox properties observed in the presence of FAD-containing mutants are largely due to dissociated cofactor.

Hydrogenases are another class of FeS cluster-containing enzymes that have been extensively characterized at electrode surfaces. The most common hydrogenases contain a catalytic cofactor (typically [NiFe] or [FeFe]) that is buried within the enzyme structure alongside accompanying FeS clusters that facilitate ET from the surface of the protein (figure 6*a*) [60–62]. These two types of hydrogenases can usually facilitate the reduction of $2H^+$ to H_2 and the oxidation of H_2 to $2H^+$, and their electrochemistry has been explored for over 30 years [63–66].

In the case of metalloenzymes that contain metallocofactors and can degrade to form various inorganic catalytic species, it is important to demonstrate that activity is from active enzyme and not from degraded cofactors or denatured proteins. In 2006, Léger and co-workers [59] investigated mutations to the ligation of the distal [4Fe–4S] cluster of hydrogenase, which is presumably the first port-of-call for ET to or from the enzyme at an electrode surface (figure 6*a*). The authors interestingly note that the k_0 of the enzyme is modified upon replacing the single His ligation of the distal cluster with a Gly, where a diminished direct bioelectrocatalytic signal is observed (figure 6*b*). Upon the addition of exogenous imidazole to the electrolyte (as a substitute for the deleted His ligating amino acid), k_0 is enhanced along with the apparent direct bioelectrocatalytic currents that are observed at the electrode. Additionally, exogenous imidazole improved the oxidative activity of the Gly mutant; however, no significant increase in oxidative activity was observed for the wild-type enzyme. These findings strongly support the hypothesis that the observed apparent direct bioelectrocatalytic response is observed from holo-enzyme, and not from denature/degraded/dissociated cofactor that is adsorbed to the electrode surface. In 2008, Lojou *et al*. demonstrated that the orientation of hydrogenase ([NiFe] from *Desulfovibrio fructosovorans*) significantly impacted the direct bioelectrocatalysis response observed at an electrode surface. Direct bioelectrocatalytic H_2-oxidation and $2H^+$-reduction currents were observed at modified gold electrode surfaces, where a combination of thiol and/or carbon nanotube modifications was employed [64]. As discussed above for the case of MCOs, orientational studies provide strong evidence to suggest that the observed bioelectrocatalytic response is in fact due to holo-enzyme.

When considering oxidoreductases that oxidize/reduce their substrate at their FAD redox cofactor, three enzymes have been deeply studied for their direct bioelectrocatalytic properties: FAD-dependent glucose dehydrogenase (FAD-GDH), cellobiose dehydrogenase (CDH) and fructose dehydrogenase (FDH). FAD-GDH has been extensively investigated as a replacement enzyme to glucose oxidase (discussed below), because it does not employ O_2 as its natural electron acceptor; thus, MET does not compete with dissolved O_2 for electrons and peroxide is not produced (from the $2e^-$ reduction of O_2) [67]. FAD-GDH has been identified from three different sources to date: Gram-negative bacteria, fungi and insects [68]. Fungal and bacterial FAD-GDH has been studied at electrode surfaces, but only the bacterial FAD-GDH has been shown to undergo DET/direct bioelectrocatalysis [69–71]. Sode and co-workers [70] have performed extensive research into the structure of this bacterial FAD-GDH (further abbreviated to bFAD-GDH in this review),

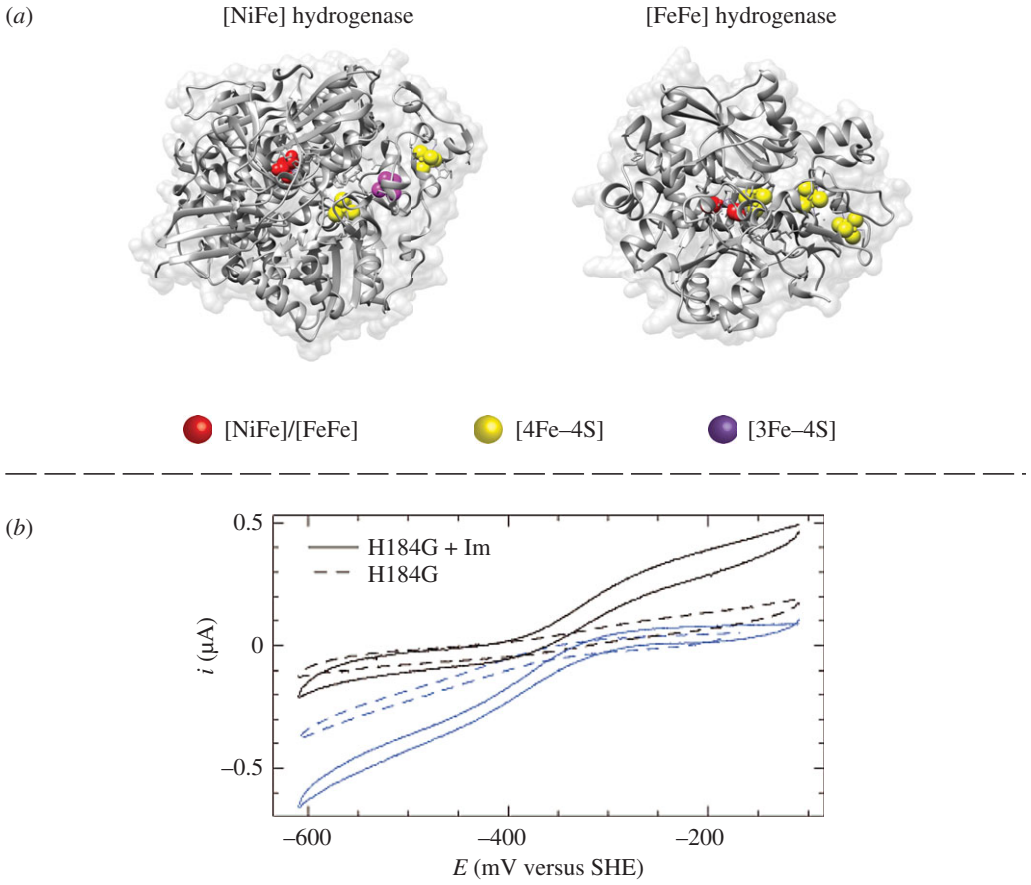

Figure 6. (*a*) Crystal structures of NiFe hydrogenase (from *Desulfovibrio vulgaris* Miyazaki F, PDB accession code: 1WUK) and FeFe hydrogenase (from *Desulfovibrio desulfuricans*, PDB accession code: 1HFE). The NiFe or FeFe catalytic centres are shown in red, the [4Fe–4S] clusters are shown in yellow and the [3Fe–4S] cluster is shown in magenta. (*b*) Direct bioelectrocatalytic H_2 oxidation and $2H^+$ reduction by NiFe hydrogenase (from *D. fructosovorans*) mutants in the absence and presence of exogenous imidazole (Im). H_2 oxidation was performed under a H_2 atmosphere (black lines), whereas $2H^+$ reduction experiments were performed under an atmosphere of Ar (blue lines, scan rate 10 mV s^{-1}, 1000 r.p.m. rotation, pH 6, 40°C). The IUPAC convention was used to plot current versus potential, where positive potentials and currents are oxidative [60]. Reprinted (adapted) with permission from [59] (copyright © 2004 American Chemical Society). (Online version in colour.)

revealing the enzyme to be a heterotrimer comprised of an FAD-containing catalytic subunit, a small chaperone subunit and a multi-haem subunit (responsible for DET). Figure 7 illustrates the structure of bFAD-GDH where glucose is oxidized and electrodes are shuttled to the electrode from the FAD cofactor via a [3Fe–4S] cluster and a multi-haem c unit.

Sode and co-workers [69] also performed a series of mutations to the FAD-harbouring domain of bFAD-GDH (from *Burkholderia cepacia*) to alter its substrate specificity, where mutants were selected for reduced reactivity with maltose oxidation, and thus more specificity towards glucose oxidation. Upon selecting a suitable mutant by traditional dye-mediated enzymatic activity assays, the direct bioelectrocatalytic activity of bFAD-GDH mutants was evaluated for glucose selectivity, providing strong information to suggest that the observed direct bioelectrocatalytic currents were due to holo-bFAD-GDH and not from dissociated FAD cofactor. In contrast with performing mutations that affect substrate specificity, it is important to investigate the integrity of direct bioelectrocatalysis by evaluating the extent to which an immobilized enzyme can still catalyse a range of natural substrates (i.e. does enzyme immobilization eliminate reactivity towards key substrates).

CDH is an enzyme that oxidizes aldoses and is commonly employed for glucose oxidation [72]. This enzyme contains an FAD-dependent dehydrogenase subunit as well as a haem-dependent subunit that is connected by a flexible peptide linker (figure 8*a*). In the literature, the ET mechanism of CDH is commonly referred to as IET because the saccharide substrate is oxidized at the FAD cofactor within the dehydrogenase subunit, from which electrons are transferred to the final electron acceptor of the enzyme via the haem subunit of the enzyme. For the purposes of this review and in the light of the wild-type CDH being comprised of the FAD dehydrogenase domain alongside the haem domain, we consider CDH to undergo direct bioelectrocatalysis. For the last 20 years or so, researchers have investigated the nature of DET between CDH and electrode surfaces, which has been concluded to be largely afforded via the haem domain (figure 8*a*) [73–77].

In early research of CDH at electrode surfaces, researchers used a protease to cleave the peptide linker of the two subunits (papain) allowing the purification of both components and subsequently their individual electrochemical analysis (figure 8*b*) [78]. Electrochemical evaluation of both of the individual subunits revealed the prominent redox peaks presented by CDH to originate from the haem subunit; following the addition of cellobiose, an oxidative response is observed that is coupled to the electrochemistry of the haem subunit, implying its role in facilitating DET from the FAD-dependent dehydrogenase domain to the electrode surface. Further, the authors reported that direct bioelectrocatalysis of cellobiose oxidation was only observed in the presence of both the

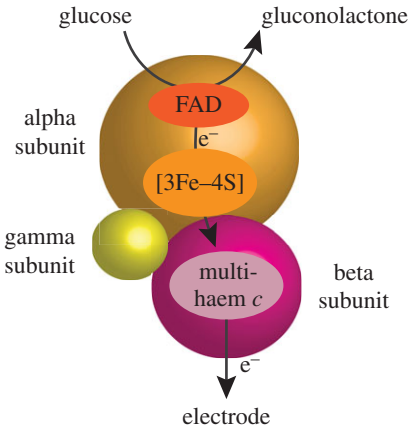

Figure 7. Proposed ET pathway of bacterial FAD-dependent glucose dehydrogenase (bFAD-GDH), as described in [64]. (Online version in colour.)

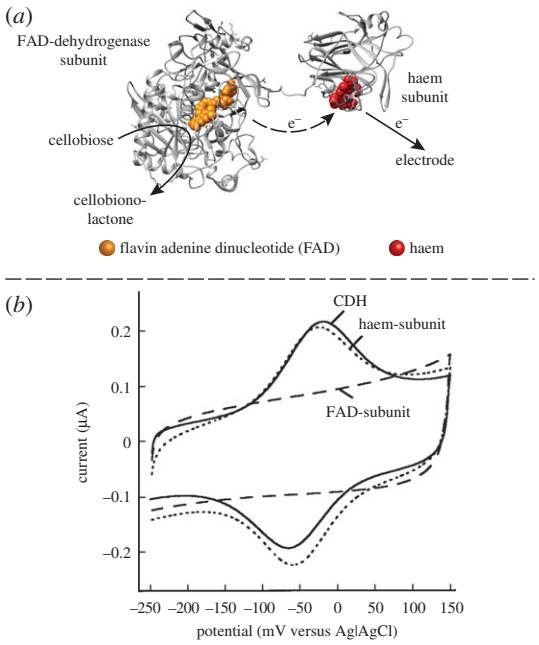

Figure 8. (*a*) Crystal structure of CDH from *N. crassa* (PDB accession code: 4QI7). The FAD cofactor is shown in orange and the haem cofactor is shown in red. Cyclic voltammetry of complete CDH (solid line), isolated FAD dehydrogenase subunit (dashed line) and isolated haem subunit (dotted line) immobilized at a gold electrode (scan rate 50 mV s^{-1}, pH 5.1 acetate buffer). The IUPAC convention was used to plot current versus potential, where positive potentials and currents are oxidative. Reprinted from [71] with permission from Elsevier. (Online version in colour.)

FAD-dependent dehydrogenase domain and the haem domain, providing further evidence that direct bioelectrocatalysis was afforded by holo-CDH and not from dissociated cofactor. Importantly, CDH is not known to produce H_2O_2, which could also be electrooxidized at the electrode surface.

A later study of CDH evaluated the effect of deglycosylation on direct bioelectrocatalysis; CDHs are typically glycosylated by about 9–16%, which is thought to limit the intimacy between CDH and an electrode surface (thereby restricting direct bioelectrocatalysis) [73]. The authors demonstrated that the deglycosylation of CDH resulted in a significant enhancement of the direct bioelectrocatalytic currents obtained for lactose oxidation, providing further evidence to support direct bioelectrocatalysis by holo-CDH and not from dissociated cofactor. The authors importantly note that direct bioelectrocatalysis was not observed for the FAD-dependent dehydrogenase subunit of CDH when separated from the haem subunit.

Researchers have studied the direct bioelectrocatalysis FAD-dependent fructose dehydrogenases from acetic acid bacteria that have a haem-containing subunit. These enzymes allow for internal relay of electrons between FAD and haem in a similar manner to CDH. The enzyme has very high specific activity and therefore has been studied for its ability to provide high current densities for sensor and fuel cell applications. The majority of the work on FAD-dependent fructose dehydrogenase has focused on high surface area electrode structures for decreasing the internal ET distance. Kano and co-workers [79] have shown that Ketjen black provides a high surface area carbon environment for facilitating DET of FAD-dependent fructose dehydrogenase. Cyclic voltammetry in the presence and absence of fructose is consistent with the potential for the haem c communicating with the electrode. Nishizawa and co-workers [80] showed that Ketjen black can be combined with different carbon fibres, cloth, etc. to produce high current density fructose bioanodes (mA cm^{-2}). Nishizawa and co-workers [81] have developed forests of carbon nanotubes for ensuring short ET distances and high current densities. Overall, this enzyme is interesting, because it readily adsorbs to carbon while maintaining high activity and this has allowed for the fabrication of high current density fructose bioanodes.

FAD-dependent dehydrogenases are not the only class of dehydrogenases that can contain haem subunits. There are three types of PQQ-dependent dehydrogenases and the type II and type III are quinohaemoproteins containing both the PQQ cofactor and at least one haem. Type II are defined as soluble, periplasmic quinohaemoproteins and type III are membrane-bound quinohaemoproteins [82]. These dehydrogenases are similar to FAD-dependent dehydrogenases in that they do not include a diffusional cofactor and can use the haem-containing subunit as a relay to internally transfer electrons to/from the electrode. Calcium ions are used to bind the PQQ cofactor in the binding site [83] and alternative ions like strontium have been used to bind the PQQ cofactor more tightly and extend the stability of the enzyme on an electrode. Of the PQQ-dependent dehydrogenases, the most common enzymes for bioelectrocatalysis are PQQ-dependent glucose dehydrogenase and alcohol dehydrogenase. It is important to note that there is a commercially available PQQ-dependent glucose dehydrogenase that is a quinoprotein that does not contain a haem, but is similar to glucose oxidase in that the cofactor is too deeply buried for direct ET. Owing to the oxygen independence of PQQ-dependent glucose dehydrogenase, it has been widely studied for mediated bioelectrocatalysis for biosensor applications, but is outside of the scope of this review due to inability for facile direct ET.

PQQ-dependent alcohol (ADH) and aldehyde (ALDH) dehydrogenases from *Gluconobacter* have been studied for bioelectrocatalysis [84–86]. These membrane-bound quinohaemoproteins have been studied for alcohol biosensing and alcohol-based EFCs [86,87]. Although PQQ-ALDH is a quinohaemoprotein and it has been used for studying the effect of orientation of the direct bioelectrocatalysis with multi-subunit proteins [88], PQQ-ADH is the more common enzyme studied electrochemically. PQQ-ADH is a three-subunit

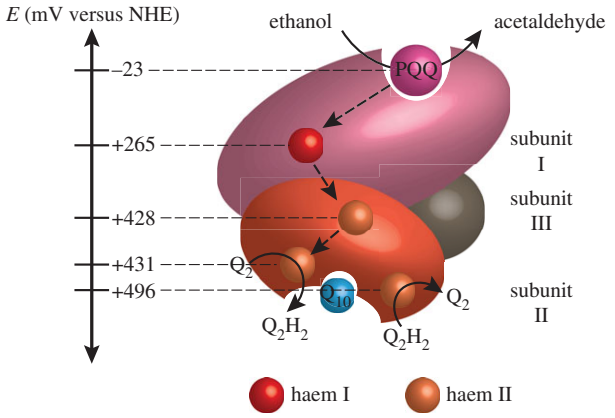

Figure 9. ET pathway of PQQ-dependent alcohol dehydrogenase (ADH) highlighting the reduction potentials of its various cofactors at pH 4.5, as described in [78]. (Online version in colour.)

quinohaemoprotein with an active subunit that contains a PQQ cofactor and a single haem c, a structural subunit that contains no cofactors and a third subunit that contains 3× haem c centres. There is a substantial loss in potential from the PQQ cofactor to the haems, but the haems provide an internal relay to transfer electrons to the electrode (figure 9) [89]. Many researchers have shown direct bioelectrocatalysis of this enzyme on a variety of electrodes, including: carbon nanotubes, glassy carbon, Toray carbon paper and polyaniline [12,90,91]. As PQQ-ADH has a multi-haem subunit that facilitates rapid internal electron relays, Sode and co-workers [92] addressed the buried cofactor of PQQ-GDH by genetically fusing the multi-haem domain of PQQ-ADH with the type 1 quinoprotein PQQ-GDH. This promoted direct ET and increased current densities.

There are several other quinohaemoproteins in the literature that have been studied for direct bioelectrocatalysis, including: PQQ-dependent aldose dehydrogenase [93], lactate dehydrogenase [94] and pyruvate dehydrogenase [95]. PQQ-dependent glycerol dehydrogenase is similar to PQQ-ADH and PQQ-ALDH, in that it is a promiscuous enzyme and it frequently loses substantial activity upon immobilization on electrode surfaces, but it has been shown to do mediated bioelectrocatalysis with either phenazine methosulfate or ferrocenylphenol [96], but up until now has shown no evidence of direct bioelectrocatalysis.

Many researchers have also investigated direct bioelectrocatalysis of cytochrome P450 and derivatives thereof. P450s are enzymes that catalyse a wide range of reactions, such as alkane hydroxylation, olefin epoxidation and dealkylation reactions, with their most common reactivity being termed 'monooxygenase' where only one O atom from O_2 is transferred to the oxidized substrate (product) [97]. The active site contains an iron(III) protoporphyrin-IX (tetradentate), which is also covalently linked to the protein via a proximal cysteine ligand. Despite the degree of research into direct bioelectrocatalysis of P450s [98], a large number of reports do not provide adequate evidence for DET.

4. Direct bioelectrocatalysis of non-metalloenzymes

The most commonly studied non-metalloenzyme for direct bioelectrocatalysis is glucose oxidase (GOx). Fungal GOx is

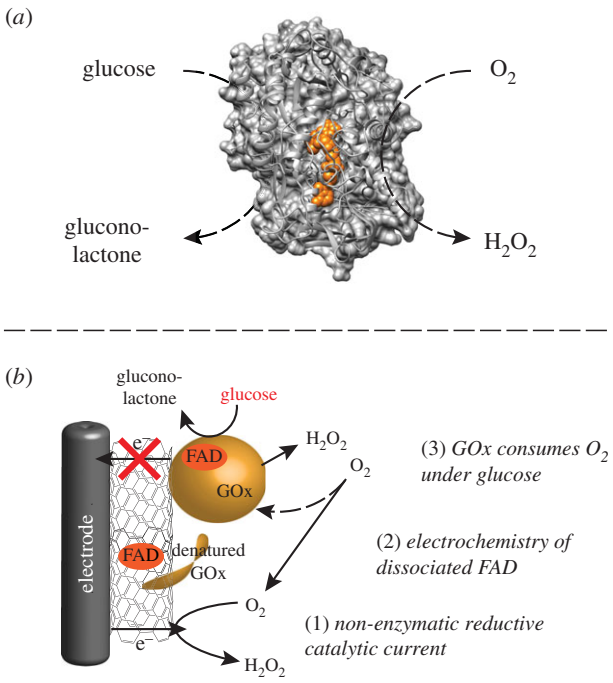

Figure 10. (*a*) Crystal structure and turnover of glucose oxidase (GOx) from *Aspergillus niger* (PDB accession code: 1GAL). (*b*) Commonly observed pseudo-DET response for GOx-modified bioelectrodes. (1) Under aerobic conditions, O_2 is reduced by the supporting electrode. (2) A pair of reversible redox peaks is observed for the FAD cofactor of GOx in the absence and presence of O_2, although it is frequently due to dissociated cofactor. (3) The addition of glucose results in the consumption of O_2 by some GOx that remains active, which yields a change in the electrochemical reduction of O_2 to H_2O_2 by the supporting electrode. (Online version in colour.)

an FAD-dependent enzyme that couples the $2e^-$ oxidation of glucose to gluconolactone with the $2e^-$ reduction of O_2 to H_2O_2 (figure 10*a*). Owing to the biotechnological desire to quantify physiological glucose concentrations for diabetes care, many researchers have attempted to develop GOx-based electrochemical devices due to the known selectivity of enzyme/substrate pairs. While a large number of devices have successfully employed polymeric materials that have been modified with redox mediators for MET, DET-based glucose strategies are frequently debated. Wooten *et al.* [99] recently evaluated the construction of a typical GOx DET-type bioelectrode, where chitosan was used as an immobilization matrix alongside carbon nanotubes. The authors observed the commonly reported characteristic responses observed for GOx DET systems, such as a reversible couple for the redox cofactor of GOx (FAD) and an amperometric response following the addition of glucose. Finally, the authors came to the conclusion that DET may not actually be taking place and that the observed electrochemistry of the FAD cofactors is most likely due to dissociated cofactor.

The most frequent pseudo-bioelectrocatalytic response observed and used as rationale to support GOx DET is: 'An enzymatic response to glucose is only observed upon the addition of glucose when O_2 is present' (figure 10*b*). Typically, researchers observe a reductive current around the potential region of the FAD cofactor of GOx, which shifts to 'less-reductive' currents upon the addition of glucose to the electrolyte, resulting in a positive shift in current magnitude. Further, researchers prepare control bioelectrodes with denatured GOx or another protein/enzyme that is inert to

glucose and this 'less-reductive' response is not observed. In this case, it is becoming more commonly agreed upon that the FAD redox response is in fact due to FAD cofactor that has dissociated from GOx and adsorbed to the electrode surface, while a portion of active GOx still remains adsorbed to the electrode surface. The reductive current arises from O_2 reduction by the supporting electrode (typically carbon, commonly modified with carbon nanotubes) and the addition of glucose results in O_2 consumption by GOx and thus less O_2 reduction by the supporting electrode.

It is important to note that the use of the terms 'anaerobic' and 'anoxic' to describe solutions in which dissolved O_2 has been displaced by purging with an inert gas is often an overstatement; trace amounts of O_2 can give rise to pseudo-glucose responses and the actual concentration of dissolved O_2 should be reported, or, work should be conducted in an anoxic chamber and the concentration of atmospheric O_2 provided. Additionally, GOx does not require O_2 to turnover glucose if a suitable electron mediator is employed (ferrocene, Os complexes, etc.) [100–102].

5. Control experiments to prove direct bioelectrocatalysis

The above review of direct bioelectrocatalysis of several metalloenzymes presents multiple approaches to confirm direct bioelectrocatalysis by a series of properly designed control experiments. This section is dedicated to summarizing and discussing experiments that can be used to differentiate direct bioelectrocatalysis from responses that arise from dissociated cofactor. It is possible, however, that a small conformational change in the enzyme takes place once the enzyme is immobilized on an electrode surface, but it is presumed that the activity of the enzyme will likely be lower due to resulting changes in the active site. Finally, a single control experiment does not always confirm direct bioelectrocatalysis and a multitude of controls should be used to confirm this ET pathway.

5.1. Product analysis

Perhaps the first port-of-call is to determine the production of the expected product of the enzymatic reaction. This does not eliminate the possibility that the reaction takes place by dissociated cofactor, although it does confirm that the reaction of interest is actually taking place. One recent example of suitable product analysis was demonstrated by Duca *et al.* [57], where an NR was co-immobilized with a noble metal catalyst to afford the stepwise reduction of NO_3^- to ammonia (NH_3) through its intermediate reduction to nitrite (NO_2^-). Initially, NO_3^- reduction to NO_2^- was confirmed by using the 'Griess assay' to detect NO_2^-, which was also correlated to the theoretical quantity of NO_2^- that should be produced by its bioelectrochemical reduction (using Coulomb's law and by calculating the charge passed during the experiment, figure 11). The authors subsequently employed noble metal catalysis to reduce the NO_2^- produced from the first step to NH_3, where a different fluorescence reagent (*o*-phthalaldehyde) was used to quantify NH_3.

Product analysis is especially important when using an enzyme that can perform the reduction in several substrates; nitrogenase, primarily an N_2-reducing enzyme, can also

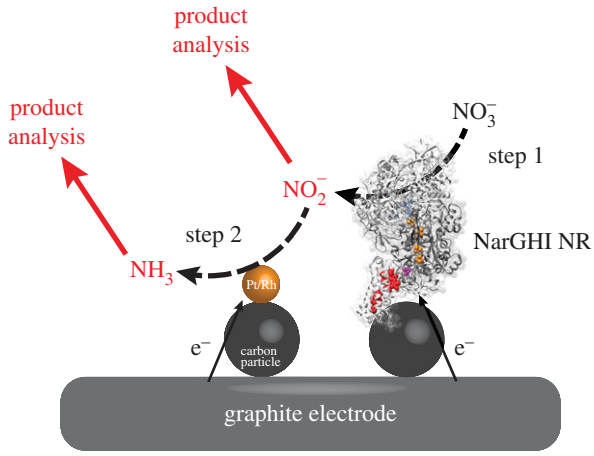

Figure 11. Duca *et al.* demonstrated the co-immobilization of NarGHI NR and Pt/Rh nanoparticles for the reduction of NO_3^- to NH_3 on a hybrid electrode, as reported in [50]. The 'Griess' assay was used to detect and quantify NO_2^- production, whereas *o*-phthalaldehyde was used to detect and quantify NH_3. (Online version in colour.)

reduce H^+, carbon dioxide (CO_2), NO_2^- and azide (N_3^-) in addition to other substrates [103]. We recently reported on the immobilized and non-immobilized electrochemistry of nitrogenase where product analysis was performed to confirm the successful production of NH_3 [26,104]. In the absence of other substrates, nitrogenase will revert to 100% H^+ reduction; thus, a catalytic current will always be present when undergoing ET.

5.2. Enzyme denaturation and non-catalytic proteins

Often, the tertiary and quaternary structures of oxidoreductases are important to their activity and these enzymes are frequently denatured at elevated temperatures (although thermostable enzymes are being increasingly investigated for improved stabilities). Enzymes can be briefly heated at elevated temperature (80–100°C for 10–30 min) to render them inactive, where their loss of activity can be evaluated following heat treatment by conventional activity assays. Additionally, proteins that are inert to the reaction of interest (such as bovine serum albumin) can be used; this is useful if the tertiary/quaternary structure of the protein is expected to be beneficial (such as in the case of immobilized films). In the event that the enzyme loses activity, it can then be used to verify direct bioelectrocatalysis, or indeed, that cofactor can dissociate from the enzyme and undergo electrocatalysis. We recently demonstrated an MET-type bioelectrode that simultaneously employed two oxidoreductases, where heat-denatured proteins were prepared to confirm the bioelectrochemical activity of each counterpart [105]. An alternative to heat denaturation would be to digest the oxidoreductase with a promiscuous protease (such as trypsin).

5.3. Inhibition of enzymatic activity

As highlighted above, direct bioelectrocatalysis by holoenzyme at an electrode surface can also be indirectly determined by initiating turnover of the substrate at the electrode followed by the addition of an inhibitor to enzymatic activity. An example of this was demonstrated by the Butt group in 2001, where NarGH NR (free of its NarI component) was studied at an electrode surface and NO_3^-

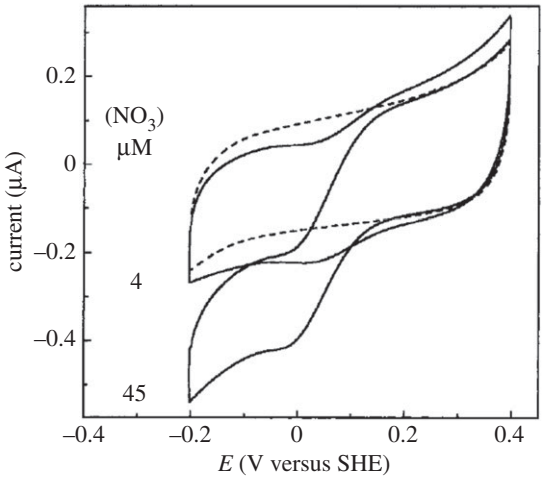

Figure 12. Direct bioelectrocatalysis of NarGH NR on a gold electrode. Electrodes were initially analysed in 4 μM of substrate (NO_3^-), which was increased to 45 μM prior to the injection of 100 μM inhibitor (N_3^-, dashed line). Scan rate 10 mV s^{-1}, 3000 r.p.m., pH 6 and 25°C [49]. Reprinted (adapted) with permission from [56] (copyright © 2004 American Chemical Society).

reduction was inhibited by the addition of N_3^- (figure 12). As discussed above for laccase and shown in figure 3, Vaz-Dominguez *et al*. demonstrated the inhibition their laccase direct bioelectrocatalytic electrodes by the addition of two different inhibitors (Cl^- and F^-). In the case of dissociated metallocofactor, inhibitors such as cyanide (CN^-) should be used with caution as CN^- could react with the dissociated metallocofactor and yield a pseudo-inhibitory response.

5.4. Mutations and modifications

Finally, perhaps the most elegant and subtle approach used to confirm possible direct bioelectrocatalysis involves the generation of mutated or modified oxidoreductases that have altered catalytic properties or properties that effect their orientation or immobilization on an electrode surface, of which a few examples were provided above. Such mutations and modifications can include single-point mutations, the cleavage of component subunits or even the deglycosylation of enzymes. If the mutation is expected to alter the catalytic properties of the enzyme, then evaluation of the apparent steady-state kinetics (i.e. Michaelis–Menten kinetics) may result in a significant change in these properties (i.e. maximum velocity, V_{MAX}, or the Michaelis constant, K_M).

Mutations can also be made to alter the mechanism of ET, or internal ET, within a protein. As outlined above, an example of this was demonstrated in 2006 by Léger and co-workers [59], who altered the ligation of the distal [4Fe–4S] cluster of a hydrogenase. As a result, the interfacial ET rate (k_0) of the enzyme at the electrode surface changed and direct bioelectrocatalysis was altered. The introduction of exogenous imidazole (presumably to replace the His residue that was replaced with a Gly residue) resulted in improved direct bioelectrocatalysis (figure 6*b*). In many cases, however, the generation of mutant enzymes is neither straightforward nor trivial.

Finally, the potential applied to the electrode may indicate whether direct bioelectrocatalysis of active enzyme is taking place, provided that the reduction potential of the enzyme's cofactor has been predetermined and that its reduction potential is not mildly altered upon any small conformational changes that may occur by immobilizing the enzyme.

6. Conclusion

This review article describes a number of metalloenzymes that have been shown to undergo internal ET to promote direct bioelectrocatalysis and the properties necessary for facile direct bioelectrocatalysis. However, the review also describes the challenges in the literature with verifying direct bioelectrocatalysis and the need for a variety of control experiments. Although mutations and modifications of the enzymes can be challenging for commercial enzyme systems, denatured controls, inhibition studies and product analysis are the required minimum experiments for evaluating direct bioelectrocatalysis.

Authors' contributions. R.D.M. and S.D.M. contributed equally and wrote the manuscript.

Competing interests. We declare we have no competing interests.

Funding. The authors would like to thank the Air Force Office of Scientific Research, USDA-NIFA and a Marie Skłodowska-Curie Individual Fellowship (Global) under the European Commission's Horizon 2020 Framework (project 654836, 'Bioelectroammonia').

References

1. Karyakin AA. 2012 Principles of direct (mediator free) bioelectrocatalysis. *Bioelectrochemistry* **88**, 70–75. (doi:10.1016/j.bioelechem.2012.05.001)
2. Leech D, Kavanagh P, Schuhmann W. 2012 Enzymatic fuel cells: recent progress. *Electrochim. Acta* **84**, 223–234. (doi:10.1016/j.electacta.2012.02.087)
3. Meredith MT, Minteer SD. 2012 Biofuel cells: enhanced enzymatic bioelectrocatalysis. *Annu. Rev. Anal. Chem.* **5**, 157–179. (doi:10.1146/annurev-anchem-062011-143049)
4. Barton SC, Gallaway J, Atanassov P. 2004 Enzymatic biofuel cells for implantable and microscale devices. *Chem. Rev.* **104**, 4867–4886. (doi:10.1021/cr020719k)
5. Bullen RA, Arnot TC, Lakeman JB, Walsh FC. 2006 Biofuel cells and their development. *Biosens. Bioelectron.* **21**, 2015–2045. (doi:10.1016/j.bios.2006.01.030)
6. Chen C, Xie Q, Yang D, Xiao H, Fu Y, Tan Y, Yao S. 2013 Recent advances in electrochemical glucose biosensors: a review. *RSC Adv.* **3**, 4473–4491. (doi:10.1039/c2ra22351a)
7. Mulchandani A, Chen W, Mulchandani P, Wang J, Rogers KR. 2001 Biosensors for direct determination of organophosphate pesticides. *Biosens. Bioelectron.* **16**, 225–230. (doi:10.1016/S0956-5663(01)00126-9)
8. Mano N, Mao F, Shin W, Chen T, Heller A. 2003 A miniature biofuel cell operating at 0.78 V. *Chem. Commun.* 518–519. (doi:10.1039/B211796G)
9. Heller A. 2004 Miniature biofuel cells. *Phys. Chem. Chem. Phys.* **6**, 209–216. (doi:10.1039/b313149a)
10. Zafar MN, Tasca F, Boland S, Kujawa M, Patel I, Peterbauer CK, Leech D, Gorton L. 2010 Wiring of pyranose dehydrogenase with osmium polymers of different redox potentials. *Bioelectrochemistry* **80**, 38–42. (doi:10.1016/j.bioelechem.2010.04.002)
11. Karyakin AA, Morozov SV, Voronin OG, Zorin NA, Karyakina EE, Fateyev VN, Cosnier S. 2007 The limiting performance characteristics in bioelectrocatalysis of hydrogenase enzymes. *Angew. Chem. Int. Ed. Engl.* **46**, 7244–7246. (doi:10.1002/anie.200701096)
12. Aquino Neto S, Suda EL, Xu S, Meredith MT, De Andrade AR, Minteer SD. 2013 Direct electron

transfer-based bioanodes for ethanol biofuel cells using PQQ-dependent alcohol and aldehyde dehydrogenases. *Electrochim. Acta* **87**, 323–329. (doi:10.1016/j.electacta.2012.09.052)

13. Vincent KA, Parkin A, Armstrong FA. 2007 Investigating and exploiting the electrocatalytic properties of hydrogenases. *Chem. Rev.* **107**, 4366–4413. (doi:10.1021/cr050191u)
14. Milton RD, Lim K, Hickey DP, Minteer SD. 2015 Employing FAD-dependent glucose dehydrogenase within a glucose/oxygen enzymatic fuel cell operating in human serum. *Bioelectrochemistry* **106**, 56–63. (doi:10.1016/j.bioelechem.2015.04.005)
15. Ó Conghaile P, Falk M, MacAodha D, Yakovleva ME, Gonaus C, Peterbauer CK, Gorton L, Shleev S, Leech D. 2016 Fully enzymatic membraneless glucose|oxygen fuel cell that provides 0.275 mA cm^{-2} in 5 mM glucose, operates in human physiological solutions, and powers transmission of sensing data. *Anal. Chem.* **88**, 2156–2163. (doi:10.1021/acs.analchem.5b03745)
16. Cosnier S, Le Goff A, Holzinger M. 2014 Towards glucose biofuel cells implanted in human body for powering artificial organs: review. *Electrochem. Commun.* **38**, 19–23. (doi:10.1016/j.elecom.2013.09.021)
17. Szczupak A, Halamek J, Halamkova L, Bocharova V, Alfonta L, Katz E. 2012 Living battery—biofuel cells operating in vivo in clams. *Energy Environ. Sci.* **5**, 8891–8895. (doi:10.1039/c2ee21626d)
18. MacVittie K, Halamek J, Halamkova L, Southcott M, Jemison WD, Lobel R, Katz E. 2013 From 'cyborg' lobsters to a pacemaker powered by implantable biofuel cells. *Energy Environ. Sci.* **6**, 81–86. (doi:10.1039/C2EE23209J)
19. Rasmussen M, Ritzmann RE, Lee I, Pollack AJ, Scherson D. 2012 An implantable biofuel cell for a live insect. *J. Am. Chem. Soc.* **134**, 1458–1460. (doi:10.1021/ja210794c)
20. Cass AEG, Davis G, Francis GD, Hill HAO, Aston WJ, Higgins IJ, Plotkin EV, Scott LDL, Turner APF. 1984 Ferrocene-mediated enzyme electrode for amperometric determination of glucose. *Anal. Chem.* **56**, 667–671. (doi:10.1021/ac00268a018)
21. Mao F, Mano N, Heller A. 2003 Long tethers binding redox centers to polymer backbones enhance electron transport in enzyme 'wiring' hydrogels. *J. Am. Chem. Soc.* **125**, 4951–4957. (doi:10.1021/ja029510e)
22. Reda T, Plugge CM, Abram NJ, Hirst J. 2008 Reversible interconversion of carbon dioxide and formate by an electroactive enzyme. *Proc. Natl Acad. Sci. USA* **105**, 10 654–10 658. (doi:10.1073/pnas.0801290105)
23. Aresta M, Dibenedetto A, Baran T, Angelini A, Łabuz P, Macyk W. 2014 An integrated photocatalytic/enzymatic system for the reduction of CO_2 to methanol in bioglycerol–water. *Beilstein J. Org. Chem.* **10**, 2556–2565. (doi:10.3762/bjoc.10.267)
24. Tan B, Hickey DP, Milton RD, Giroud F, Minteer SD. 2015 Regeneration of the NADH cofactor by a rhodium complex immobilized on multi-walled carbon nanotubes. *J. Electrochem. Soc.* **162**, H102–H107. (doi:10.1149/2.0111503jes)
25. Reeve HA, Ash PA, Park H, Huang A, Posidias M, Tomlinson C, Lenz O, Vincent KA. 2017 Enzymes as modular catalysts for redox half-reactions in H_2-powered chemical synthesis: from biology to technology. *Biochem. J.* **474**, 215–230. (doi:10.1042/bcj20160513)
26. Milton RD, Cai R, Abdellaoui S, Leech D, DeLacey AL, Pita M, Minteer SD. 2017 Bioelectrochemical Haber–Bosch process: an ammonia-producing H_2/N_2 fuel cell. *Angew. Chem. Int. Ed.* **56**, 2680–2683. (doi:10.1002/anie.201612500)
27. Milton RD, Hickey DP, Abdellaoui S, Lim K, Wu F, Tan B, Minteer SD. 2015 Rational design of quinones for high power density biofuel cells. *Chem. Sci.* **6**, 4867–4875. (doi:10.1039/C5SC01538C)
28. Ghindilis AL, Atanasov P, Wilkins E. 1997 Enzyme-catalyzed direct electron transfer: fundamentals and analytical applications. *Electroanalysis* **9**, 661–674. (doi:10.1002/elan.1140090902)
29. Marcus RA, Sutin N. 1985 Electron transfers in chemistry and biology. *Biochim. Biophys. Acta* **811**, 265–322. (doi:10.1016/0304-4173(85)90014-X)
30. Abdellaoui S, Corgier BC, Mandon CA, Doumèche B, Marquette CA, Blum LJ. 2013 Biomolecules immobilization using the aryl diazonium electrografting. *Electroanalysis* **25**, 671–684. (doi:10.1002/elan.201200334)
31. Berezin IV, Bogdanovskaya VA, Varfolomeev SD, Tarasevich MR, Yaropolov AI. 1978 Equilibrium oxygen potential in the presence of laccase. *Dokl. Akad. Nauk SSR* **240**, 615–618.
32. Blanford CF, Foster CE, Heath RS, Armstrong FA. 2008 Efficient electrocatalytic oxygen reduction by the 'blue' copper oxidase, laccase, directly attached to chemically modified carbons. *Faraday Discuss.* **140**, 319–335. (doi:10.1039/b808939f)
33. Cracknell JA, McNamara TP, Lowe ED, Blanford CF. 2011 Bilirubin oxidase from *Myrothecium verrucaria*: X-ray determination of the complete crystal structure and a rational surface modification for enhanced electrocatalytic O_2 reduction. *Dalton Trans.* **40**, 6668–6675. (doi:10.1039/c0dt01403f)
34. Mano N. 2012 Features and applications of bilirubin oxidases. *Appl. Microbiol. Biotechnol.* **96**, 301–307. (doi:10.1007/s00253-012-4312-9)
35. Shleev S, Tkac J, Christenson A, Ruzgas T, Yaropolov AI, Whittaker JW, Gorton L. 2005 Direct electron transfer between copper-containing proteins and electrodes. *Biosens. Bioelectron.* **20**, 2517–2554. (doi:10.1016/j.bios.2004.10.003)
36. Solomon EI, Sundaram UM, Machonkin TE. 1996 Multicopper oxidases and oxygenases. *Chem. Rev.* **96**, 2563–2605. (doi:10.1021/cr9500460)
37. Quintanar L, Stoj C, Taylor AB, Hart PJ, Kosman DJ, Solomon EI. 2007 Shall we dance? How a multicopper oxidase chooses its electron transfer partner. *Acc. Chem. Res.* **40**, 445–452. (doi:10.1021/ar600051a)
38. Hong G, Ivnitski DM, Johnson GR, Atanassov P, Pachter R. 2011 Design parameters for tuning the Type 1 Cu multicopper oxidase redox potential: insight from a combination of first principles and empirical molecular dynamics simulations. *J. Am. Chem. Soc.* **133**, 4802–4809. (doi:10.1021/ja105586q)
39. Brocato S, Lau C, Atanassov P. 2012 Mechanistic study of direct electron transfer in bilirubin oxidase. *Electrochim. Acta* **61**, 44–49. (doi:10.1016/j.electacta.2011.11.074)
40. Vaz-Dominguez C, Campuzano S, Rudiger O, Pita M, Gorbacheva M, Shleev S, Fernandez VM, De Lacey AL. 2008 Laccase electrode for direct electrocatalytic reduction of O_2 to H_2O with high-operational stability and resistance to chloride inhibition. *Biosens. Bioelectron.* **24**, 531–537. (doi:10.1016/j.bios.2008.05.002)
41. Blanford CF, Heath RS, Armstrong FA. 2007 A stable electrode for high-potential, electrocatalytic O_2 reduction based on rational attachment of a blue copper oxidase to a graphite surface. *Chem. Commun.* 1710–1712. (doi:10.1039/b703114a)
42. Meredith MT, Minson M, Hickey D, Artyushkova K, Glatzhofer DT, Minteer SD. 2011 Anthracene-modified multi-walled carbon nanotubes as direct electron transfer scaffolds for enzymatic oxygen reduction. *ACS Catal.* **1**, 1683–1690. (doi:10.1021/cs200475q)
43. Giroud F, Minteer SD. 2013 Anthracene-modified pyrenes immobilized on carbon nanotubes for direct electroreduction of O_2 by laccase. *Electrochem. Commun.* **34**, 157–160. (doi:10.1016/j.elecom.2013.06.006)
44. Karaśkiewicz M, Nazaruk E, Żelechowska K, Biernat JF, Rogalski J, Bilewicz R. 2012 Fully enzymatic mediatorless fuel cell with efficient naphthylated carbon nanotube–laccase composite cathodes. *Electrochem. Commun.* **20**, 124–127. (doi:10.1016/j.elecom.2012.04.011)
45. Mano N, Edembe L. 2013 Bilirubin oxidases in bioelectrochemistry: features and recent findings. *Biosens. Bioelectron.* **50**, 478–485. (doi:10.1016/j.bios.2013.07.014)
46. Krishnan S, Armstrong FA. 2012 Order-of-magnitude enhancement of an enzymatic hydrogen-air fuel cell based on pyrenyl carbon nanostructures. *Chem. Sci.* **3**, 1015–1023. (doi:10.1039/C2SC01103D)
47. Gutierrez-Sanchez C, Ciaccafava A, Blanchard PY, Monsalve K, Giudici-Orticoni MT, Lecomte S, Lojou E. 2016 Efficiency of enzymatic O_2 reduction by *Myrothecium verrucaria* bilirubin oxidase probed by surface plasmon resonance, PMIRRAS, and electrochemistry. *ACS Catal.* **6**, 5482–5492. (doi:10.1021/acscatal.6b01423)
48. Milton RD, Giroud F, Thumser AE, Minteer SD, Slade RCT. 2014 Bilirubin oxidase bioelectrocatalytic cathodes: the impact of hydrogen peroxide. *Chem. Commun.* **50**, 94–96. (doi:10.1039/c3cc47689h)
49. Lalaoui N, LeGoff A, Holzinger M, Cosnier S. 2015 Fully oriented bilirubin oxidase on porphyrin-functionalized carbon nanotube electrodes for electrocatalytic oxygen reduction. *Chem. Eur. J.* **21**, 16 868–16 873. (doi:10.1002/chem.201502377)

50. Salaj-Kosla U, Poeller S, Schuhmann W, Shleev S, Magner E. 2013 Direct electron transfer of *Trametes hirsuta* laccase adsorbed at unmodified nanoporous gold electrodes. *Bioelectrochemistry* **91**, 15–20. (doi:10.1016/j.bioelechem.2012.11.001)
51. Dagys M *et al.* 2017 Oxygen electroreduction catalysed by laccase wired to gold nanoparticles via the trinuclear copper cluster. *Energy Environ. Sci.* **10**, 498–502. (doi:10.1039/C6EE02232D)
52. Léger C, Jones AK, Albracht SPJ, Armstrong FA. 2002 Effect of a dispersion of interfacial electron transfer rates on steady state catalytic electron transport in [NiFe]-hydrogenase and other enzymes. *J. Phys. Chem. B* **106**, 13 058–13 063. (doi:10.1021/jp0265687)
53. Elliott SJ, Hoke KR, Heffron K, Palak M, Rothery RA, Weiner JH, Armstrong FA. 2004 Voltammetric studies of the catalytic mechanism of the respiratory nitrate reductase from *Escherichia coli*: how nitrate reduction and inhibition depend on the oxidation state of the active site. *Biochemistry* **43**, 799–807. (doi:10.1021/bi035869j)
54. Hille R, Hall J, Basu P. 2014 The mononuclear molybdenum enzymes. *Chem. Rev.* **114**, 3963–4038. (doi:10.1021/cr400443z)
55. Frangioni B, Arnoux P, Sabaty M, Pignol D, Bertrand P, Guigliarelli B, Léger C. 2004 In *Rhodobacter sphaeroides* respiratory nitrate reductase, the kinetics of substrate binding favors intramolecular electron transfer. *J. Am. Chem. Soc.* **126**, 1328–1329. (doi:10.1021/ja0384072)
56. Anderson LJ, Richardson DJ, Butt JN. 2001 Catalytic protein film voltammetry from a respiratory nitrate reductase provides evidence for complex electrochemical modulation of enzyme activity. *Biochemistry* **40**, 11 294–11 307. (doi:10.1021/bi002706b)
57. Duca M, Weeks JR, Fedor JG, Weiner JH, Vincent KA. 2015 Combining noble metals and enzymes for relay cascade electrocatalysis of nitrate reduction to ammonia at neutral pH. *ChemElectroChem* **2**, 1086–1089. (doi:10.1002/celc.201500166)
58. Kalimuthu P, Ringel P, Kruse T, Bernhardt PV. 2016 Direct electrochemistry of nitrate reductase from the fungus *Neurospora crassa*. *Biochim. Biophys. Acta Bioenerg.* **1857**, 1506–1513. (doi:10.1016/j.bbabio.2016.04.001)
59. Dementin S, Belle V, Bertrand P, Guigliarelli B, Adryanczyk-Perrier G, De Lacey AL, Fernandez VM, Rousset M, Léger C. 2006 Changing the ligation of the distal 4Fe4S cluster in NiFe hydrogenase impairs inter- and intramolecular electron transfers. *J. Am. Chem. Soc.* **128**, 5209–5218. (doi:10.1021/ja060233b)
60. Lubitz W, Ogata H, Rüdiger O, Reijerse E. 2014 Hydrogenases. *Chem. Rev.* **114**, 4081–4148. (doi:10.1021/cr4005814)
61. Armstrong FA, Belsey NA, Cracknell JA, Goldet G, Parkin A, Reisner E, Vincent KA, Wait AF. 2009 Dynamic electrochemical investigations of hydrogen oxidation and production by enzymes and implications for future technology. *Chem. Soc. Rev.* **38**, 36–51. (doi:10.1039/B801144N)
62. De Lacey AL, Fernández VM, Rousset M, Cammack R. 2007 Activation and inactivation of hydrogenase function and the catalytic cycle: spectroelectrochemical studies. *Chem. Rev.* **107**, 4304–4330. (doi:10.1021/cr0501947)
63. Yaropolov AI, Karyakin AA, Varfolomeev SD, Berezin IV. 1984 Mechanism of H_2-electrooxidation with immobilized hydrogenase. *Bioelectrochem. Bioenerg.* **12**, 267–277. (doi:10.1016/0302-4598(84)87009-9)
64. Lojou E, Luo X, Brugna M, Candoni N, Dementin S, Giudici-Orticoni MT. 2008 Biocatalysts for fuel cells: efficient hydrogenase orientation for H_2 oxidation at electrodes modified with carbon nanotubes. *J. Biol. Inorg. Chem.* **13**, 1157–1167. (doi:10.1007/s00775-008-0401-8)
65. Léger C, Dementin S, Bertrand P, Rousset M, Guigliarelli B. 2004 Inhibition and aerobic inactivation kinetics of *Desulfovibrio fructosovorans* NiFe hydrogenase studied by protein film voltammetry. *J. Am. Chem. Soc.* **126**, 12 162–12 172. (doi:10.1021/ja046548d)
66. Rüdiger O, Gutiérrez-Sánchez C, Olea D, Pereira IA.C., Vélez M, Fernández VM, DeLacey AL. 2010 Enzymatic anodes for hydrogen fuel cells based on covalent attachment of Ni-Fe hydrogenases and direct electron transfer to SAM-modified gold electrodes. *Electroanalysis* **22**, 776–783. (doi:10.1002/elan.200880002)
67. Tsujimura S, Kojima S, Kano K, Ikeda T, Sato M, Sanada H, Omura H. 2006 Novel FAD-dependent glucose dehydrogenase for a dioxygen-insensitive glucose biosensor. *Biosci. Biotechnol. Biochem.* **70**, 654–659. (doi:10.1271/bbb.70.654)
68. Ferri S, Kojima K, Sode K. 2011 Review of glucose oxidases and glucose dehydrogenases: a bird's eye view of glucose sensing enzymes. *J. Diabetes Sci. Technol.* **5**, 1068–1076. (doi:10.1177/193229681100500507)
69. Yamashita Y, Ferri S, Huynh ML, Shimizu H, Yamaoka H, Sode K. 2013 Direct electron transfer type disposable sensor strip for glucose sensing employing an engineered FAD glucose dehydrogenase. *Enzyme Microb. Technol.* **52**, 123–128. (doi:10.1016/j.enzmictec.2012.11.002)
70. Shiota M, Yamazaki T, Yoshimatsu K, Kojima K, Tsugawa W, Ferri S, Sode K. 2016 An Fe–S cluster in the conserved Cys-rich region in the catalytic subunit of FAD-dependent dehydrogenase complexes. *Bioelectrochemistry* **112**, 178–183. (doi:10.1016/j.bioelechem.2016.01.010)
71. Kakehi N, Yamazaki T, Tsugawa W, Sode K. 2007 A novel wireless glucose sensor employing direct electron transfer principle based enzyme fuel cell. *Biosens. Bioelectron.* **22**, 2250–2255. (doi:10.1016/j.bios.2006.11.004)
72. Ludwig R, Harreither W, Tasca F, Gorton L. 2010 Cellobiose dehydrogenase: a versatile catalyst for electrochemical applications. *ChemPhysChem* **11**, 2674–2697. (doi:10.1002/cphc.201000216)
73. Ortiz R, Matsumura H, Tasca F, Zahma K, Samejima M, Igarashi K, Ludwig R, Gorton L. 2012 Effect of deglycosylation of cellobiose dehydrogenases on the enhancement of direct electron transfer with electrodes. *Anal. Chem.* **84**, 10 315–10 323. (doi:10.1021/ac3022899)
74. Tasca F, Harreither W, Ludwig R, Gooding JJ, Gorton L. 2011 Cellobiose dehydrogenase aryl diazoniunn modified single walled carbon nanotubes: enhanced direct electron transfer through a positively charged surface. *Anal. Chem.* **83**, 3042–3049. (doi:10.1021/ac103250b)
75. Coman V, Ludwig R, Harreither W, Haltrich D, Gorton L, Ruzgas T, Shleev S. 2010 A direct electron transfer-based glucose/oxygen biofuel cell operating in human serum. *Fuel Cells* **10**, 9–16. (doi:10.1002/fuce.200900121)
76. Tasca F, Gorton L, Harreither W, Haltrich D, Ludwig R, Noll G. 2009 Comparison of direct and mediated electron transfer for cellobiose dehydrogenase from *Phanerochaete soridida*. *Anal. Chem.* **81**, 2791–2798. (doi:10.1021/ac900225z)
77. Coman V, Vaz-Dominguez C, Ludwig R, Herreither W, Haltrich D, De Lacey AL, Ruzgas T, Gorton L, Shleev S. 2008 A membrane-, mediator-, cofactor-less glucose/oxygen biofuel cell. *Phys. Chem. Chem. Phys.* **10**, 6093–6096. (doi:10.1039/b808859d)
78. Lindgren A, Larsson T, Ruzgas T, Gorton L. 2000 Direct electron transfer between the heme of cellobiose dehydrogenase and thiol modified gold electrodes. *J. Electroanal. Chem.* **494**, 105–113. (doi:10.1016/S0022-0728(00)00326-0)
79. Kamitaka Y, Tsujimura S, Kano K. 2007 High current density bioelectrolysis of D-fructose at fructose dehydrogenase-adsorbed and Ketjen black-modified electrodes without a mediator. *Chem. Lett.* **36**, 218–219. (doi:10.1246/cl.2007.218)
80. Haneda K, Yoshino S, Ofuji T, Miyake T, Nishizawa M. 2012 Sheet-shaped biofuel cell constructed from enzyme-modified nanoengineered carbon fabric. *Electrochim. Acta* **82**, 175–178. (doi:10.1016/j.electacta.2012.01.112)
81. Miyake T, Yoshino S, Yamada T, Hata K, Nishizawa M. 2011 Self-regulating enzyme-nanotube ensemble films and their application as flexible electrodes for biofuel cells. *J. Am. Chem. Soc.* **133**, 5129–5134. (doi:10.1021/ja111517e)
82. Toyama H, Mathews FS, Adachi O, Matsushita K. 2004 Quinohemoprotein alcohol dehydrogenases: structure, function, and physiology. *Arch. Biochem. Biophys.* **428**, 10–21. (doi:10.1016/j.abb.2004.03.037)
83. Matsushita K, Toyama H, Yamada M, Adachi O. 2002 Quinoproteins: structure, function, and biotechnological applications. *Appl. Microbiol. Biotechnol.* **58**, 13–22. (doi:10.1007/s00253-001-0851-1)
84. Razumiene J, Niculescu M, Ramanavicius A, Laurinavicius V, Csöregi E. 2002 Direct bioelectrocatalysis at carbon electrodes modified with quinohemoprotein alcohol dehydrogenase from *Gluconobacter* sp. 33. *Electroanalysis* **14**, 43–49. (doi:10.1002/1521-4109(200201)14:1<43::AID-ELAN43>3.0.CO;2-5)
85. Ramanavicius A, Habermüller K, Csöregi E, Laurinavicius V, Schuhmann W. 1999 Polypyrrole-entrapped quinohemoprotein alcohol dehydrogenase. Evidence for direct electron transfer

via conducting-polymer chains. *Anal. Chem.* **71**, 3581–3586. (doi:10.1021/ac981201c)

86. Aquino Neto S, Hickey DP, Milton RD, De Andrade AR, Minteer SD. 2015 High current density PQQ-dependent alcohol and aldehyde dehydrogenase bioanodes. *Biosens. Bioelectron.* **72**, 247–254. (doi:10.1016/j.bios.2015.05.011)
87. Ramanavicius A, Kausaite A, Ramanaviciene A. 2005 Biofuel cell based on direct bioelectrocatalysis. *Biosens. Bioelectron.* **20**, 1962–1967. (doi:10.1016/j.bios.2004.08.032)
88. Xu S, Minteer SD. 2013 Investigating the impact of multi-heme pyrroloquinoline quinone-aldehyde dehydrogenase orientation on direct bioelectrocatalysis via site specific enzyme immobilization. *ACS Catal.* **3**, 1756–1763. (doi:10.1021/cs400316b)
89. Tkac J, Svitel J, Vostiar I, Navratil M, Gemeiner P. 2009 Membrane-bound dehydrogenases from *Gluconobacter* sp.: interfacial electrochemistry and direct bioelectrocatalysis. *Bioelectrochemistry* **76**, 53–62. (doi:10.1016/j.bioelechem.2009.02.013)
90. Treu BL, Arechederra R, Minteer SD. 2009 Bioelectrocatalysis of ethanol via PQQ-dependent dehydrogenases utilizing carbon nanomaterial supports. *J. Nanosci. Nanotechnol.* **9**, 2374–2380. (doi:10.1166/jnn.2009.SE33)
91. Schubart IW, Goebel G, Lisdat F. 2012 A pyrroloquinolinequinone-dependent glucose dehydrogenase (PQQ-GDH) electrode with direct electron transfer based on polyaniline modified carbon nanotubes for biofuel cell applications. *Electrochim. Acta* **82**, 224–232. (doi:10.1016/j.electacta.2012.03.128)
92. Okuda J, Yamazaki T, Fukasawa M, Kakehi N, Sode K. 2007 The application of engineered glucose dehydrogenase to a direct electron-transfer-type continuous glucose monitoring system and a compartmentless biofuel cell. *Anal. Lett.* **40**, 431–440. (doi:10.1080/00032710600964692)
93. Tursula S, Lau C, Atanassov P, Smolander M, Minteer SD. 2012 Characterization and stability study of immobilized PQQ-dependent aldose dehydrogenase bioanodes. *Electroanalysis* **24**, 229–238. (doi:10.1002/elan.201100546)
94. Treu BL, Minteer SD. 2008 Isolation and purification of PQQ-dependent lactate dehydrogenase from *Gluconobacter* and use for direct electron transfer at carbon and gold electrodes. *Bioelectrochemistry* **74**, 73–77. (doi:10.1016/j.bioelechem.2008.07.005)
95. Treu BL, Sokic-Lazic D, Minteer SD. 2010 Bioelectrocatalysis of pyruvate with PQQ-dependent pyruvate dehydrogenase. *ECS Trans.* **25**, 1–11. (doi:10.1149/1.3309672)
96. Lapenaite I, Kurtinaitiene B, Razumiene J, Laurinavicius V, Marcinkeviciene L, Bachmatova I, Meskys R, Ramanavicius A. 2005 Properties and analytical application of PQQ-dependent glycerol dehydrogenase from *Gluconobacter* sp. 33. *Anal. Chim. Acta* **549**, 140–150. (doi:10.1016/j.aca.2005.06.025)
97. Meunier B, de Visser SP, Shaik S. 2004 Mechanism of oxidation reactions catalyzed by cytochrome P450 enzymes. *Chem. Rev.* **104**, 3947–3980. (doi:10.1021/cr020443g)
98. Fleming BD, Johnson DL, Bond AM, Martin LL. 2006 Recent progress in cytochrome P450 enzyme electrochemistry. *Expert Opin. Drug Metab. Toxicol.* **2**, 581–589. (doi:10.1517/17425255.2.4.581)
99. Wooten M, Karra S, Zhang M, Gorski W. 2014 On the direct electron transfer, sensing, and enzyme activity in the glucose oxidase/carbon nanotubes system. *Anal. Chem.* **86**, 752–757. (doi:10.1021/ac403250w)
100. Milton RD, Giroud F, Thumser AE, Minteer SD, Slade RCT. 2013 Hydrogen peroxide produced by glucose oxidase affects the performance of laccase cathodes in glucose/oxygen fuel cells: FAD-dependent glucose dehydrogenase as a replacement. *Phys. Chem. Chem. Phys.* **15**, 19 371–19 379. (doi:10.1039/c3cp53351d)
101. Prévoteau A, Mano N. 2013 How the reduction of O_2 on enzymes and/or redox mediators affects the calibration curve of 'wired' glucose oxidase and glucose dehydrogenase biosensors. *Electrochim. Acta* **112**, 318–326. (doi:10.1016/j.electacta.2013.08.173)
102. Tremey E, Suraniti E, Courjean O, Gounel S, Stines-Chaumeil C, Louerat F, Mano N. 2014 Switching an O_2 sensitive glucose oxidase bioelectrode into an almost insensitive one by cofactor redesign. *Chem. Commun.* **50**, 5912–5914. (doi:10.1039/C4CC01670J)
103. Burgess BK, Lowe DJ. 1996 Mechanism of molybdenum nitrogenase. *Chem. Rev.* **96**, 2983–3012. (doi:10.1021/cr950055x)
104. Milton RD, Abdellaoui S, Khadka N, Dean DR, Leech D, Seefeldt LC, Minteer SD. 2016 Nitrogenase bioelectrocatalysis: heterogeneous ammonia and hydrogen production by MoFe protein. *Energy Environ. Sci.* **9**, 2550–2554. (doi:10.1039/C6EE01432A)
105. Holade Y, Yuan M, Milton RD, Hickey DP, Sugawara A, Peterbauer CK, Haltrich D, Minteer SD. 2017 Rational combination of promiscuous enzymes yields a versatile enzymatic fuel cell with improved coulombic efficiency. *J. Electrochem. Soc.* **164**, H3073–H3082. (doi:10.1149/2.0111703jes)